Monte Carlo study of structural ordering in charged colloids using a long-range attractive interaction

B. V. R. Tata* and Norio Ise†
Central Laboratory, Rengo Company Limited, 186-1-4 Ohhiraki, Fukushima, Osaka 553, Japan
(Received 21 July 1997; revised manuscript received 1 April 1998)

Monte Carlo simulations have been carried out for aqueous charged colloidal suspensions interacting via an effective pair potential $U_s(r)$, which has the long-range attractive term in addition to the usual screened Coulomb repulsion. Simulations are performed over four orders of magnitude of particle volume fractions (ϕ) under salt free as well as added salt conditions. The computed pair correlation functions $g(r)$ at high values of ϕ show a face centered cubic (fcc) crystalline order, which is found to transform to a body centered cubic (bcc) crystalline order upon lowering of ϕ. The crystalline order is found to melt into a liquidlike order upon the addition of salt. A purely repulsive potential based on Derjaguin-Landau-Vervey-Overbeek theory was earlier claimed to be responsible for the formation of bcc and fcc phases and the associated order-disorder transitions. It is clearly shown here that $U_s(r)$ also explains equally well such phenomena and the results are shown to be in close agreement with experimental observations. Simulations in the dilute regime show a vapor-liquid transition upon variation of ϕ and the coexistence of ordered and disordered regions with voids upon variation of the charge on the particles. These results explain the reported experimental observations, which suggested the existence of a long-range attraction in the interparticle interaction. For very low volume fractions calculated pair correlation functions show only a single peak and are found to be independent of ϕ. The reported results on the direct measurement of the pair potential are discussed in the light of the present results.
[S1063-651X(98)09508-7]

PACS number(s): 82.70.Dd, 64.70.Pf

I. INTRODUCTION

The electrostatically stabilized aqueous monodisperse colloids exhibit crystalline, liquidlike, and even glassy structural ordering at ambient conditions [1] depending on the suspension parameters such as the particle concentration n_p, salt concentration C_s, effective charge Ze, and diameter d of the particle. The perfect scaling of the magnitudes of elastic constants, the latent heat of melting of colloidal crystals with particle concentration, and the interaction energy being the same order as in atomic systems have made the researchers treat monodispersed colloids as model condensed matter systems [1]. Apart from the interest in fundamental studies, the colloidal crystals have important technological uses as optical devices [2] and materials with photonic band gaps [3]. The advantage of this model system is that the range and strength of interparticle interaction can be varied over a wide range rather easily. It is believed that the interaction can be described using the Derjaguin-Landau-Verwey-Overbeek (DLVO) theory [4]. The DLVO potential is predominantly screened Coulomb repulsion, except at very short distances (of the order of a few angstroms where the van der Waals attraction is dominant). In stable suspensions the van der Waals attraction is negligible; hence hereafter we refer to the screened Coulomb repulsion as the DLVO potential. During the past several years more and more experimental evidence has emerged for the existence of an attractive interaction at large interparticle separations (of the order of micrometers). Some of these are (a) stable voids in colloidal fluids and crystals [1,5–11], (b) the nonspace filling localized ordered structures coexisting with disordered regions [12,13], and (c) highly ordered colloidal single crystals [14]. Here the measured interparticle distance D_{expt} is found to be significantly smaller than the average interparticle distance D_0 obtained from n_p, suggesting the nonspace filling nature of the ordered phase. A system of particles interacting via a purely repulsive interaction, when restricted to a finite volume, cannot lead to a large difference in the interparticle distance making the suspensions inhomogeneous. The importance of the attractive interaction was demonstrated by the (d) observation of reentrant transition [1,15] when the salt concentration C_s alone is varied and (e) the vapor-liquid condensation upon variation of n_p at a fixed salt concentration [1,16]. (f) Observation of long-lived metastable colloidal crystallites [17] and (g) amorphous dense regions coexisting with voids in highly charged dilute poly(chlorostyrene-styrene sulfonate) suspensions [18] also attest to the presence of long-range attraction. All these observations cannot be explained using the DLVO potential. We mention here that this evidence is on suspensions at finite volume fractions ϕ. However, there have been experimental reports of direct measurement of pair potentials on very dilute suspensions under confined [19–22] as well as unconfined geometries [23,24]. A pair potential obtained under confined geometry reportedly shows a long-range attraction.

In view of the above experimental results and the limitations of the DLVO theory, several authors have attempted to describe charged colloidal suspensions by (a) taking into ac-

*Permanent address: Materials Science Division, Indira Gandhi Centre for Atomic Research, Kalpakkam 603102, Tamil Nadu, India.
†Author to whom correspondence should be addressed.

count ionic correlations [25,26], (b) modeling the fluctuations in the surface charge on the particles due to adsorption and disorption of small ions [27], and (c) treating the asymmetry in size and charge between colloidal particles using integral equation theories [28,29]. Although the interparticle interaction resulting from these model calculations shows the existence of attraction, either the range of attraction is found to be short [27] or analytical forms are not available [28,29] for further studies. Sogami and Ise [30] have proposed an effective interaction model based on the Gibbs free energy of the interaction. This model not only takes into account the large size difference between colloidal particles and small ions but also relates the variation of macroion charge to the release of counterions. The important result of this model is that the effective pair potential $U_s(r)$ has an attractive minimum at interparticle distances of several thousands of angstroms, which is consistent with the experimental evidence mentioned above. The well depth U_m and position R_m strongly depend on the screening parameter κ. The presence of this secondary minimum has led to controversy for some time [31,32]. Overbeek's arguments that brought out the controversy are shown to be incorrect by Ise *et al.* [33], Smalley [34], and Schmitz [35–37].

We mention here that experimental structure factors of liquidlike ordered colloidal suspensions [38], data of elastic constants [39] and photothermal compression [40] of colloidal crystals, reentrant transitions [1,41], and the coexistence of voids with ordered and disordered regions [18,42] have been explained successfully using $U_s(r)$. However, it has not been shown whether this potential explains successfully the formation of fcc and bcc phases and the associated order-disorder transitions. Similarly, the reported experimental observation of the transition from the vapor-liquid coexistence to homogeneous liquidlike order upon variation of ϕ under deionized conditions is not yet explained. Our aim is to explain these results by performing simulations for measured suspension parameters using $U_s(r)$. Further, it is also of interest to study the systematic dependence of structural ordering on volume fraction ϕ, charge density σ, and salt concentration C_s. Hence we carry out Monte Carlo (MC) simulations with $U_s(r)$ by varying these parameters over a wide range. The equilibrium state of the suspension is characterized by calculating the pair correlation function $g(r)$, coordinate-averaged pair correlation function $g_c(r)$, and mean square displacement $\langle r^2 \rangle$. The results are organized in this paper as follows.

The details of MC simulations are given in Sec. II. Section III deals with simulation results at high volume fractions, where suspensions are expected to be homogeneous [i.e., the interparticle separation D_s obtained from first peak position in $g(r)$ being equal to the average interparticle separation D_0 obtained from ϕ] and ordered. Section IV describes the simulation results at intermediate volume fractions. The experimental results that suggested the existence of a long-range attraction are discussed in this section. Section V presents the simulation results for a very dilute regime of the suspensions and the results on the direct measurement of the pair potential. A brief summary with conclusions are given in Sec. VI.

II. DETAILS OF SIMULATION

MC simulations are carried out using the Metropolis algorithm with periodic boundary conditions for a canonical ensemble (at constant N, V, and T, where N, V, and T are, respectively, the number of particles, volume, and temperature). The particles in aqueous suspensions of spherical particles are assumed to interact via a pair potential $U_s(r)$ [30], which has the form

$$U_s(r) = 2\frac{(Ze)^2}{\epsilon}\left(\frac{\sinh(\kappa d/2)}{\kappa d}\right)^2\left(\frac{A}{r}-\kappa\right)\exp(-\kappa r), \quad (1)$$

where $A = 2 + \kappa d \coth(\kappa d/2)$ and the inverse Debye screening length κ is given as

$$\kappa^2 = 4\pi e^2(n_p Z + C_s)/\epsilon k_B T. \quad (2)$$

The diameter d of the particle is taken to be 110 nm. Ze is the effective charge on the particle (related to the surface charge density by $\sigma = Ze/\pi d^2$), C_s is the salt concentration, T is the temperature (298 K), ϵ is the dielectric constant of water, and k_B is the Boltzmann constant. The position of the potential minimum R_m is given as $R_m = \{A + [A(A+4)]^{1/2}\}/2\kappa$ and its depth by $U_m = U_s(R_m)$. Both R_m and U_m depend on σ and C_s. For the required volume fraction ϕ ($\phi = n_p \pi d^3/6$), the length l of the MC cell is fixed from the relation $l^3 = N/n_p$.

In the high volume fraction regime suspensions are expected to order into a fcc or bcc crystalline order depending on the value of ϕ and other suspension parameters. In order to find out the true ordered state we carry out simulations with different system sizes and initial configurations being liquidlike, bcc, and fcc. Slowing down of the MC evolution process (the rate at which the system reaches equilibrium from the initial configuration) can take place when the simulation parameters are close to the phase transition [43,44]. In such a situation it is known that monitoring the height of the first peak in the structure factor $S_{\max}$ along with the total interaction energy U_T is useful in finding out unambiguously whether or not the system has reached thermal equilibrium. Hence, along with U_T, $S_{\max}$ also is monitored during the evolution of the system from ordered states. Most of the simulations away from the transition (e.g., melting) take approximately 4×10^5 configurations to reach equilibrium, while those close to the transition need nearly 8×10^6 configurations. A Monte Carlo Step (MCS) is defined as the set of N configurations during which, on average, each particle gets a chance to move. The step size to move the particles during the MC evolution process is chosen in such a way that the trial acceptance ratio is always around 50% [46]. Simulation results reported here correspond to a true equilibrium state as we perform simulations with widely different initial configurations evolving to the same final state [43–45]. By performing simulations for the same set of parameters with $N = 250$, 432, and 1024, we find that the results are the same within statistical error for $N \geqslant 432$. Hence N is fixed at 432. After reaching equilibrium $g(r)$, $g_c(r)$, $S_{\max}$, and the mean square displacement $\langle r^2 \rangle$ are calculated using procedures reported earlier [1,41,45].

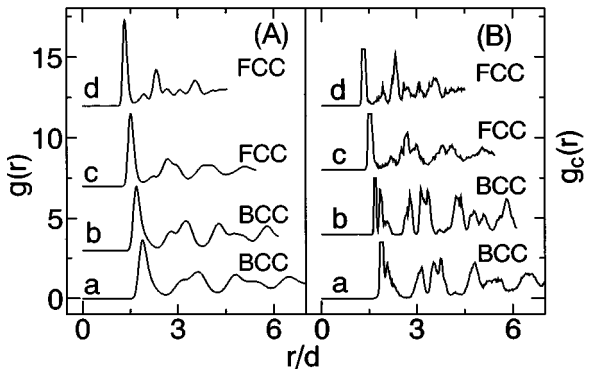

FIG. 1. (A) $g(r)$ versus r at high volume fractions for suspension parameters $C_s=0$ and $\sigma=0.15\ \mu\text{C/cm}^2$. Curves a, b, c, and d correspond to $\phi=0.1$, 0.14, 0.2, and 0.3 respectively. Curves b, c, and d are shifted vertically for the sake of clarity. (B) $g_c(r)$ versus r for the same suspension parameters as in (A) and the first peak height of curves a, b, c, and d are 10.2, 11.8, 9.5, and 8.3, respectively. The curves b, c, and d are shifted vertically for the sake of clarity.

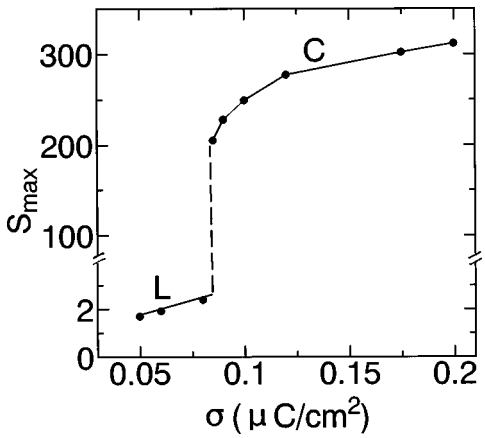

FIG. 2. $S_{\max}$ as a function of surface charge density on the particles. The sharp increase in its value is due to the $L\rightarrow C$ transition. The suspension parameters are $\phi=0.03$ and $C_s=0$.

III. HOMOGENEOUS SUSPENSION: FCC AND BCC ORDERING AND MELTING TRANSITION

There have been reports of experimental phase diagrams for polystyrene suspensions consisting of fcc, bcc, and liquidlike phases [1,47]. The convenient experimental parameters are the volume fraction ϕ and salt concentration C_s. The screened Coulomb repulsive potential given by the DLVO theory is claimed to be responsible for the ordering and has been used extensively to understand the ordering phenomena and associated phase transitions [1,45,48–51]. In this section we show simulations carried out for high volume fractions using $U_s(r)$ under salt free as well as added salt conditions. The simulations are started from disordered (liquidlike) states, which are prepared by performing simulations at high salt concentrations. After reaching equilibrium pair correlation functions are calculated and are shown in Fig. 1. The coordinate-averaged pair correlation function [1,45] $g_c(r)$ obtained by averaging the coordinates of the particles over a sufficiently large number of configurations is free from thermal broadening and helps in identifying the crystal structure unambiguously. Hence $g_c(r)$ is also calculated and is shown in Fig. 1(B). It is clear from Fig. 1 that for low values of ϕ suspensions exhibit a bcc crystalline order and upon increasing the volume fraction a fcc order. Hence the bcc to fcc transition for salt free conditions is expected to take place in between the values of $\phi=0.14$ and 0.20. Indeed, the experimental observation of Sirota *et al.* [47] showed a bcc structure for volume fractions below 0.15 and a fcc structure above 0.2. Thus there exists a close agreement between our simulations and experiments. bcc as well as fcc crystalline order is found to melt into a liquidlike order upon increasing the salt concentration. The fcc structure that occurs at higher volume fraction melted at a higher value of C_s than the bcc crystalline structure. This salt dependence is the same as that reported in the experiments [47].

In order to identify the crystal-liquid transition we carried out simulations for different values of C_s. For these simulations the initial configuration is always chosen to be particles arranged on a bcc lattice as the volume fraction used for these simulations is rather low $\phi=0.03$, where suspensions are expected to form only a bcc crystalline structure. The $S_{\max}$ and the $\langle r^2\rangle$ as functions of MCS are calculated using equilibrium particle positions as described in our earlier papers [1,45]. The melting trnasition has been identified from the sudden change in $S_{\max}$ behavior as a function of C_s, which occurred at $C_s=6.5\ \mu M$. Further, $S_{\max}$ is found to be as high as 2.8 just before freezing, which is consistent with the Hansen-Verlet criterion of freezing reported for atomic [52] and colloidal systems [1,45,48,49]. The ratio of the root mean square displacement to the lattice spacing W is found to be 0.27 ± 0.05, which is consistent with the Lindemann criterion [53] for melting reported earlier for colloidal systems [1,45].

The charge density σ of the particle plays an important role in determining the ordering of the charge stabilized suspensions as it alters the range and strength of the interaction. In the case of polystyrene colloids, a variation in σ is possible by controlling the concentration of charge determining salts during synthesis. In the case of charge stabilized silica colloids, σ can be varied by controlling the sodium hydroxide concentration [54]. The pair correlation functions for different σ values with $C_s=0$ showed liquidlike behavior at low values of $\sigma(<0.08\ \mu\text{C/cm}^2)$ and crystalline behavior for larger values of σ. The transition is identified by computing $S_{\max}$ as a function of σ and is shown in Fig. 2. The sudden change in $S_{\max}$ occurring at $\sigma=0.085\ \mu\text{C/cm}^2$ is due to the freezing transition driven by σ. We mention here that the value of $\sigma=0.085\ \mu\text{C/cm}^2$ at the crystal-liquid transition is in close agreement with that reported by Yamanaka *et al.* [54] for aqueous silica colloidal suspensions.

Simulations are performed as a function of ϕ, keeping other suspension parameters fixed to investigate the effect of the variation in the interparticle separation on the structural ordering. The calculated pair correlation functions are shown in Fig. 3. As expected, the first peak position in $g(r)$ shifts to lower r values and is due to the increase in n_p. Further, a liquidlike order (curves a and b of Fig. 3) can be seen for low values of ϕ and crystalline order (curves c and d of Fig. 3) upon increasing ϕ. The freezing transition is identified

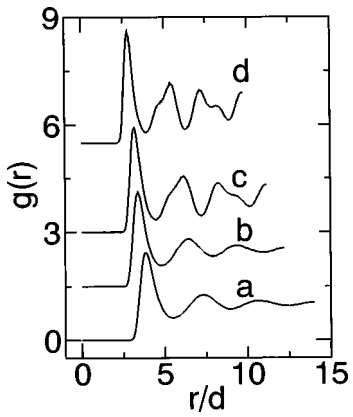

FIG. 3. $g(r)$ versus r for different intermediate values of volume fraction ϕ. Curves a, b, c, and d correspond to $\phi = 0.01, 0.015, 0.02$, and 0.03, respectively. Curves b, c, and d are shifted vertically for the sake of clarity. The other suspension parameters are $\sigma = 0.2\ \mu C/cm^2$ and $C_s = 4\ \mu M$.

from the behavior of S_{max} as a function of ϕ and is found to occur at $\phi = 0.0175$. When the volume fraction is increased, the strength of the interaction between particles increases, which leads to the buildup of structural correlations. The freezing takes place whenever the structural correlations cross a threshold value.

Until now, the DLVO potential alone had been claimed to be responsible for the observed structural ordering and associated phase transitions in charge stabilized colloids. However, present simulations thus clearly demonstrate that $U_s(r)$, which has the long-range attractive term in addition to usual screened Coulomb repulsive term, also explains equally well the same phenomenon. It is easy to understand from Table I and Fig. 4 why $U_s(r)$ is also successful in explaining the structural ordering and the associated transitions. Table I shows that the suspensions obey the relation $D_0 \geqslant R_m$ except at very high values of C_s. Here D_0 is the average interparticle separation calculated using the expression $D_0 = P(1/n_p)^{1/3}$ (where $P = 1.0911$ for bcc order and 1.1266 for fcc order) and the values of ϕ. Since the structure is also known from simulations, we also estimate the average interparticle separation D_s using the first peak position of $g(r)$. The ratio D_s/D_0 is found to be one for the suspension parameters listed in Table I. This suggests that suspensions are homogeneous (occupying the full volume). Further, it can be seen from Fig. 4 (see also Table I) that $R_m \leqslant D_0$. Thus the particles that are at D_0 experience only a screened Coulomb repulsion and the strength of the interaction at D_0 determines the structural ordering. Since the attraction is not dominant $U_s(r)$ also explains equally well the structural ordering and the associated order-disorder transitions in homogeneous suspensions. In these suspensions, which of the two pair potentials better describe the observed phenomenon is difficult to judge because accurate measurements of σ and C_s are experimentally not easy.

IV. INHOMOGENEOUS SUSPENSIONS: VAPOR-LIQUID COEXISTENCE AND VOIDS WITH ORDERED AND DISORDERED REGIONS

In the preceding section we presented results on homogeneous suspensions where the interparticle interaction is dominated by a repulsive term. In this section we discuss simulation results for dilute suspensions where the attractive part plays an important role in determining the structure and its need in explaining experimental evidence that suggested the long-range attraction in the effective interparticle interaction.

For dilute aqueous polystyrene suspensions Tata *et al.* [1,16] have reported a phase transition analogous to the well known vapor-liquid condensation in atomic systems. Upon deionization, weakly interacting homogeneous suspensions below a critical particle concentration condense into a concentrated phase with liquidlike order and a dilute vapor phase. Arora *et al.* [1,15] have reported that above a critical concentration suspensions that are homogeneous and noninteracting at high salt concentrations exhibit vapor-liquid condensation for the intermediate salt concentrations and reenter a homogeneous state having liquidlike order at low salt con-

TABLE I. Inverse Debye screening length (κ), position of the potential minimum (R_m), depth of the potential well (U_m), and average interparticle separation (D_0) for different suspension parameters at high volume fractions. The abbreviations fcc, bcc, and L represent the face centered cubic, body centered cubic crystalline, and liquid states, respectively

ϕ	σ ($\mu C/cm^2$)	C_s (μM)	κd	R_m/d	U_m/k_BT	D_0/d	State
0.30	0.15	0	4.092	1.737	0.591	1.352	fcc
0.30	0.15	50	4.830	1.614	0.495	1.352	fcc
0.30	0.15	65	5.030	1.587	0.471	1.352	fcc
0.30	0.15	160	6.149	1.476	0.356	1.352	fcc
0.30	0.15	350	7.926	1.369	0.237	1.352	L
0.25	0.15	0	3.736	1.737	0.639	1.437	fcc
0.25	0.15	250	6.846	1.427	0.302	1.437	L
0.20	0.15	0	3.341	1.931	0.689	1.547	fcc
0.20	0.15	30	3.888	1.781	0.619	1.547	fcc
0.20	0.15	200	6.123	1.478	0.358	1.547	L
0.14	0.15	0	2.795	2.152	0.742	1.742	bcc
0.14	0.15	10	3.022	2.049	0.723	1.742	bcc
0.14	0.15	140	5.123	1.576	0.460	1.742	L
0.03	0.2	0	1.494	3.478	1.177	2.83	bcc
0.03	0.2	4	1.661	3.179	1.240	2.83	bcc
0.03	0.2	6	1.739	3.061	1.263	2.83	bcc
0.03	0.2	6.5	1.757	3.034	1.269	2.83	L
0.03	0.2	7	1.776	3.008	1.274	2.83	L
0.03	0.2	8	1.813	2.958	1.283	2.83	L
0.03	0.2	10	1.884	2.867	1.299	2.83	L
0.03	0.2	15	2.051	2.683	1.328	2.83	L
0.03	0.085	0	0.974	5.121	0.159	2.83	bcc
0.03	0.085	0.1	0.981	5.088	0.160	2.83	bcc
0.03	0.085	0.4	1.001	4.994	0.163	2.83	bcc
0.03	0.085	1	1.039	4.820	0.167	2.83	L
0.03	0.085	2	1.101	4.570	0.175	2.83	L
0.03	0.05	0	0.747	6.590	0.0442	2.83	L
0.03	0.06	0	0.818	6.039	0.069	2.83	L
0.03	0.09	0	1.002	4.986	0.183	2.83	bcc
0.03	0.1	0	1.057	4.748	0.235	2.83	bcc
0.03	0.12	0	1.157	4.366	0.361	2.83	bcc
0.03	0.175	0	1.398	3.687	0.868	2.83	bcc

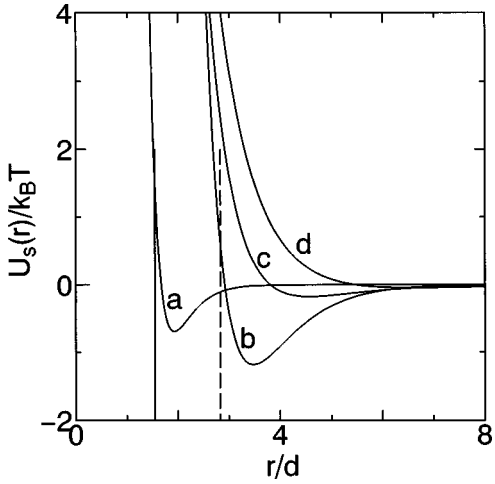

FIG. 4. Pair potential $U_s(r)/k_BT$ for different suspension parameters. Curves a and b correspond to the same values of $\sigma = 0.15\ \mu\text{C/cm}^2$ and $C_s = 0$, but volume fractions 0.2 and 0.03, respectively. Curves c and d correspond to the same values of $\phi = 0.03$ but σ and C_s are $0.085\ \mu\text{C/cm}^2$, $2\ \mu M$, and $0.05\ \mu\text{C/cm}^2$, $0\ \mu M$, respectively. The vertical continuous and dotted lines denote the average interparticle spacing D_0 corresponding to values of $\phi = 0.2$ and 0.03, respectively.

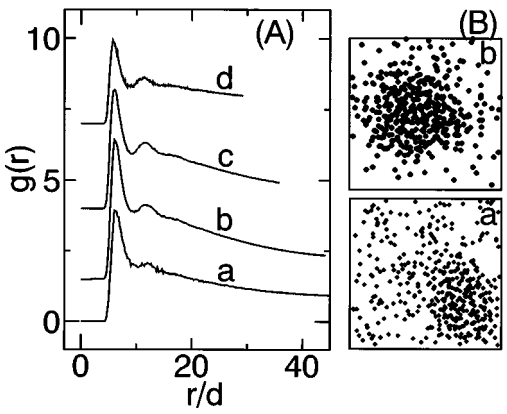

FIG. 5. (A) $g(r)$ vs r for dilute suspensions for different values of ϕ with $\sigma = 0.21\ \mu\text{C/cm}^2$ and $C_s = 4\ \mu M$. Curves a, b, c, and d correspond to $\phi = 0.25\times10^{-3}$, 0.32×10^{-3}, 0.60×10^{-3}, and 1.12×10^{-3}, respectively. Curves b, c, and d are shifted vertically for the sake of clarity. (B) Projection of the particle coordinates in the MC cell. The parameters of a and b are the same as $g(r)$ for curves b and d, respectively.

centration. $U_s(r)$ has been shown earlier to explain the salt driven reentrant transition [1,41].

Here we report MC simulation results performed as a function of ϕ for a fixed salt concentration, with an aim to understand the experimental observations of Tata *et al.* [1,16]. We mention here that some of the suspension parameters used in the simulations are the same as those reported by Tata *et al.* [16] and are given in Table II. The calculated pair correlation functions and the projection of the particle coordinates for different values of ϕ are shown in Figs. 5 and 6. It can be seen in Fig. 5 that the $g(r)$ for ϕ values in the range (0.25×10^{-3})–(1.12×10^{-3}) are markedly different from those at (2.27×10^{-3})–(4.0×10^{-3}) (Fig. 6). The first peak and a few other peaks at higher r suggest structural correlations up to several neighbor distances. Unlike for the homogeneous suspensions, the first peak position in $g(r)$ at these volume fractions occur very close to the potential minimum R_m. Further, the pair correlation functions decay to one gradually as r increases. This type of behavior is expected only when the suspensions are inhomogeneous. The appearance of peaks in pair correlation functions at distances much shorter than D_0 together with a liquidlike structural correlation suggests the formation of dense phase droplets. The projection of the particles in the MC cell [Fig. 5(b)] shows the formation of liquidlike droplets coexisting with isolated particles that constitute the rare phase. Thus suspensions in the ϕ range (0.25×10^{-3})–(1.12×10^{-3}) can be identified as the vapor-liquid coexisting state. Increasing ϕ beyond 1.12×10^{-3} showed typical liquidlike behavior as shown in Fig. 6. The projection of the coordinates in the MC cell [Fig. 6(B)] also appears homogeneous. Thus present simulations agree well with the experimental observation

TABLE II. Inverse Debye screening length (κ), position of the potential minimum (R_m), depth of the potential well (U_m), and average interparticle separation (D_0) for different dilute suspensions. The abbreviations VL and L represent the vapor-liquid coexisting state, and liquid state, respectively.

ϕ (units of 10^{-3})	σ (μC/cm^2)	C_s (μM)	κd	R_m/d	U_m/k_BT	D_0/d	State
0.20	0.21	4	0.736	6.682	0.770	15.03	VL
0.25	0.21	4	0.739	6.659	0.772	13.96	VL
0.32	0.21	4	0.743	6.630	0.780	12.85	VL
0.60	0.21	4	0.757	6.504	0.790	10.43	VL
1.12	0.21	4	0.784	6.290	0.810	8.46	VL
1.60	0.21	4	0.807	6.118	0.833	7.52	VL
2.27	0.21	4	0.839	5.896	0.861	6.69	L
2.86	0.21	4	0.866	5.720	0.884	6.19	L
3.40	0.21	4	0.890	5.575	0.772	5.85	L
4.00	0.21	4	0.916	5.426	0.926	5.53	L
9.00	0.21	4	1.109	4.540	1.073	4.22	L
10.0	0.21	4	1.143	4.414	1.097	4.08	L
15.0	0.21	4	1.303	3.922	1.198	3.57	L

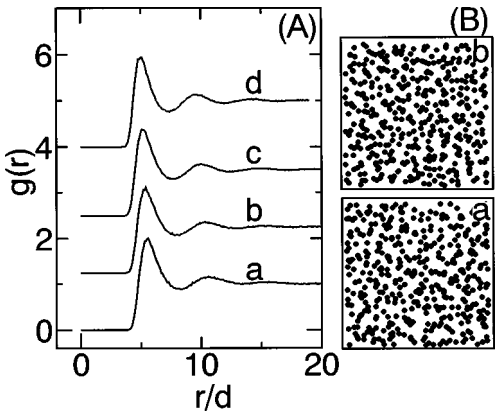

FIG. 6. (A) $g(r)$ vs r for dilute suspensions with higher values of ϕ keeping other parameters the same as those in Fig. 5. Curves a, b, c, and d correspond to $\phi=2.27\times10^{-3}$, 2.86×10^{-3}, 3.40×10^{-3}, and 4.0×10^{-3}, respectively. Curves b, c, and d are shifted vertically for the sake of clarity. (B) Projection of the particle coordinates in the MC cell. The parameters of a and b are the same as $g(r)$ for curves b and d, respectively.

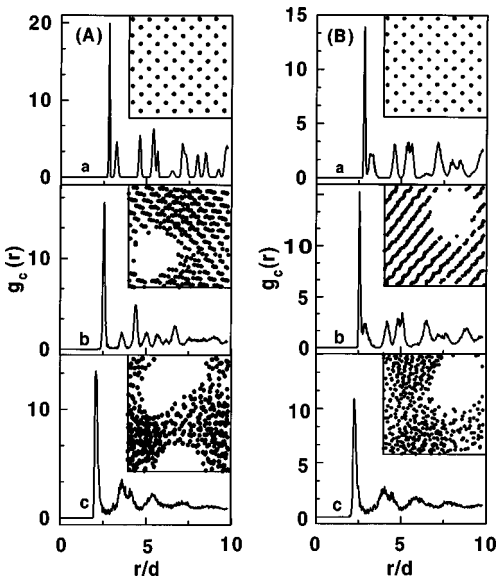

FIG. 7. (A) $g_c(r)$ vs r for suspensions for different σ at $C_s=0$ and $\phi=0.03$. Curves a, b, and c correspond to $\sigma=0.2$, 0.4, and 0.68 μC/cm^2, respectively. The projections of the time-averaged particle coordinates in the MC cell are shown in the insets. (B) $g_c(r)$ for suspensions with different salt concentrations for $\sigma=0.35$ μC/cm^2 and $\phi=0.03$. Curves a, b, and c correspond to $C_s=0$, 2, and 15 μM, respectively. The insets correspond to projections of the time averaged particle coordinates in the MC cell.

[16] of vapor-liquid coexistence at values of $\phi<2.0\times10^{-3}$ and the appearance of a homogeneous state having liquidlike order upon increasing ϕ under low salt concentrations. The vapor-liquid coexistence at low values of ϕ ($\phi<0.2\times10^{-3}$) occurs when R_m is smaller than D_0 (see Table II) and $U_m\approx1k_BT$. Under these conditions the particles that are initially at D_0 get trapped in the potential well with R_m as the average interparticle distance constituting the condensed phase. Since the well depths are only of the order of k_BT, all particles are not expected to get trapped. Those particles that remained untrapped constitute the gas phase. Further, one can also see from Table II that the difference R_m-D_0 monotonically decreases as ϕ is increased. The suspensions exhibit a vapor-liquid coexistence for large differences and a homogeneous liquidlike structure when the difference is very small or positive.

For large well depths ($U_m>2k_BT$) and when $R_m<D_0$, suspensions can be inhomogeneous. From Eq. (1) it can be seen that well depths are large when the charge on the particles is high. We have carried out systematic investigations of the effect of σ on the structural ordering and the results are reported in our earlier paper [42] and hence we discuss it only briefly here. Figure 7 shows the effect of σ and C_s on structural ordering for dilute suspensions. For a suspension with $\sigma=0.2$ μC/cm^2 and $C_s=0$ [Fig. 7(A)] the simulations show a homogeneous crystalline order (bcc). Upon increasing the charge on the particles suspensions become inhomogeneous in the form of a dense phase coexisting with voids. The structural ordering within the dense phase depends on the value of σ and C_s. The homogeneous to inhomogeneous transition is identified and discussed in detail elsewhere [42]. There exists a critical charge density below which the suspensions are homogeneous and ordered. Above the critical charge density suspensions become inhomogeneous. Shown in Fig. 7(B) is the effect of salt concentration on a suspension whose charge density is just below the critical charge density. It can be seen that a homogeneous crystalline order existing at $C_s=0$ becomes inhomogeneous upon increasing the salt concentration. The ordering within the dense phase of the inhomogeneous state depends on the amount of salt present in the suspension. Thus observation of a homogeneous ordered state or a void structure coexisting with ordered-disordered regions depend on the suspension parameters. The charge on the particles and the salt concentration in the suspensions play an important role in determining the structural ordering as well as homogeneity of the suspensions. The present simulation results explain reported experimental observations of a homogeneous crystalline state [1,47] as well as inhomogeneous phases in the form of voids with ordered or disordered (amorphous) regions [1,7,9,11]. When well depths are large compared to k_BT and $R_m<D_0$, particles that are initially at a separation of D_0 get trapped strongly into the potential well, resulting in the formation of a dense phase with interparticle separation close to R_m. As the total volume of the suspension is fixed the fraction of the volume f_v [$f_v=1-(R_m/D_0)^3$] appears in the form of voids. Our recent experiments on highly charged poly(chlorostyrene-styrene sulfonate) particles have shown voids coexisting with dense amorphous regions, confirming the existence of large well depths at several particle diameters, when particles are highly charged [18,42]. Such an observation is analogous to the gas-solid coexistence in atomic systems. It is clear from these simulations that a κ-dependent long-range attractive term in addition to the usual repulsive term explains consistently all the experimental observations. On the other hand, the theoretical calculations of van Roij and Hansen [55] show that the gas-solid and the gas-liquid coexistence can also occur even with a purely repulsive screened Coulomb pair potential, provided the effective Hamiltonian contains a negative term that can

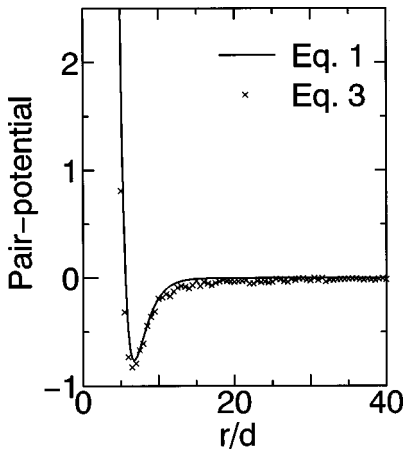

FIG. 8. Pair potential in units of k_BT obtained using Eqs. (1) and (3) for suspension parameters $\phi=1.0\times10^{-5}$, $\sigma=0.21$ μC/cm^2, and $C_s=4$ μM.

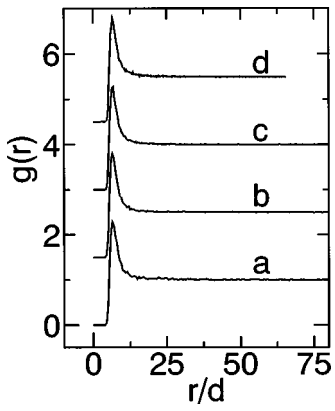

FIG. 9. $g(r)$ vs r for very dilute suspensions for different values of ϕ. The values of σ and C_s are the same as those in Fig. 7. Curves a, b, c, and d correspond to $\phi=0.1\times10^{-4}$, 0.3×10^{-4}, 0.60×10^{-4}, and 1.0×10^{-4}, respectively. Curves b, c, and d are shifted vertically for the sake of clarity.

drive a spinodal instability. The negative term arises due to the macroion-counterion interaction. However, the quantitative agreement between the experimental results and the calculations using the effective Hamiltonian for physically reasonable suspension parameters has yet to be demonstrated. Further, the reentrant transition [15] reported in dilute suspensions as a function of C_s are difficult to understand using van Roij and Hansen's calculations [55].

V. SIMULATIONS AT VERY LOW VOLUME FRACTIONS

In this section we discuss the MC simulation results carried out at very low volume fractions [$\phi=(0.1\times10^{-4})$–(1.0×10^{-4})] with an aim to understand the recent measurements of the interparticle interaction in charged colloids under very dilute conditions [19,21–23]. For sufficiently dilute dispersions the relationship

$$g(r)=\exp[-U(r)/k_BT] \tag{3}$$

can be used to obtain the pair potential $U(r)$ [56]. In order to check whether the volume fractions used here satisfy this relation, we use $g(r)$ obtained from simulations and Eq. (3). As expected, the pair potential $U(r)$ (see Fig. 8) obtained at these low volume fractions is found to be the same as that used initially to obtain $g(r)$ in simulations. This suggests that at very low volume fractions suspensions obey Eq. (3) and the interaction between particles is the true pair potential. Pair correlation functions calculated for such dilute suspensions are shown in Fig. 9. Table III summarizes the suspension parameters and the simulation results. It can be seen that there exists only a single peak occurring at the distance $r=R_m$ and no further peaks at large r, suggesting that the suspensions are noninteracting [gaslike (G)]. Further, the peak position is found to be independent of ϕ even when the particle concentration is varied over one order of magnitude. This suggests that in this range of volume fractions suspensions are essentially noninteracting. Kepler and Fraden (KF) have observed such a concentration independence (see Fig. 2 of Ref. [19]) in their experiments and their pair correlation functions also showed a single peak. KF [19] as well as Crocker and Grier (CG) [22] employed Eq. (3) to obtain the pair potential $U(r)$, which indeed showed the existence of a long-range attraction when the gap between like-charged glass plates used for confining the suspension is about $<6\mu$m. These suspensions are called confined colloids.

However, when the gap is $>7\mu$m, the measured $U(r)$ shows no attraction [22]. CG attribute the absence of an attraction to the absence of confinement and interpret the data corresponding to about 8μm as direct evidence for the DLVO pair potential but not to $U_s(r)$ based on the effective charge numbers Z and κ extracted by fitting to the expression of the DLVO potential and $U_s(r)$. Further, CG have not performed independent measurements for Z, C_s, and n_p, which characterize the suspensions used for $U(r)$ measurements.

We have carried out careful effective charge measure-

TABLE III. Inverse Debye screening length (κ), position of the potential minimum (R_m), depth of the potential well (U_m), and average interparticle separation (D_0) for very dilute suspensions. The abbreviation G represents the gaseous state.

ϕ (units of 10^{-4})	σ (μC/cm^2)	C_s (μM)	κd	R_m/d	U_m/k_BT	D_0/d	State
0.1	0.21	4	0.726	6.772	0.760	40.82	G
0.3	0.21	4	0.727	6.762	0.761	28.30	G
0.6	0.21	4	0.728	6.743	0.763	22.46	G
1.0	0.21	4	0.732	6.729	0.765	18.95	G

ments [57] on the same suspensions (i.e., catalog numbers and the suppliers are the same) used by CG. Surprisingly, these direct measurements revealed that the effective charge numbers are much smaller than those mentioned by CG in Ref. [22]. In addition to such a disagreement in the charge, we notice that the $U(r)$ data on confined colloids is not completely free from the effects of confinement. The evidence in support of our claim is described below.

Recently, Muromato *et al.* [58] have investigated, using a confocal laser scanning microscope, which probes much higher depths than the conventional optical microscope used by CG, the effect of a like-charged glass plate on the distribution of charged colloidal spheres in dilute suspensions for different charge densities of the glass plate and for different salt concentrations of the suspensions. These results clearly show that the particle concentration is high close (<10 μm) to the glass plate and gradually decreases to an average concentration far away from the plate. Muromato *et al.* [58] call this enhancement in the particle concentration close to the glass plate a gathering of particles near a like-charged plate. These observations suggest that the plate-particle interaction is significant and persists to distances as high as 5–50 μm depending on the charge. In light of the observations of Muromato *et al.*, we believe that CG's $U(r)$ data corresponding to about an 8-μm gap need not be entirely free from confinement.

To summarize, CG's $U(r)$ data corresponding to about a gap of 8μm is not entirely free from geometrical confinement of the glass plates. These observations, together with our measurements of Z on their particles, which show a large discrepancy with respect to their estimated values, lead us to conclude that CG's $U(r)$ measurements corresponding to about an 8-μm separation do not provide compelling evidence for the nonexistence of attraction in dilute charged colloids and the failure of $U_s(r)$ to describe them.

Our experimental observations, viz., the vapor-liquid condensation in dilute suspensions seen as a function of volume fraction [16] and as a function of salt concentration [15], for low charge density particles and the coexistence of voids with glasslike disordered regions [18] in dilute suspensions with high charge density particles, suggest that the charge density on the particles dictates the strength of the long-range attraction seen in the bulk dilute suspensions. The position of the well depth is dictated by small ion concentration (i.e., counterion concentration n_pZ plus salt ion concentration C_s). Since the counterion concentration depends on the charge on the particle, the range of the attraction also depends on the charge density of the particle. It is easy to conclude from these observations that the long-range attraction at very dilute concentrations is observable only when colloidal particles are highly charged. Yoshino's observation of long-lived colloidal pairs provides such evidence [59].

The fact is that the colloidal particles used by CG [22] are not highly charged and hence there is no measurable attraction in $U(r)$ for a greater than 7μm gap of the glass plates. However, this does not rule out the applicability of $U_s(r)$ to explain their observation of the screened Coulomb repulsion in the measured $U(r)$. It is easy to see from Eq. (1) that $U_s(r)$ has a screened Coulomb repulsive term, which is the same as that of the DLVO potential except for the prefactor. For very dilute suspensions with low charge density particles the well depths become too small to be detected experimentally. In such cases $U_s(r)$ also behaves more like the DLVO potential. Hence the observed $U(r)$ can be fitted to both $U_s(r)$ and the DLVO potential. In fact, CG have done this and extracted the values for Z and κ. Further, we could also fit $U_s(r)$ to CG's experimental $U(r)$ data reported earlier [24]. This fit gave us a well depth of $0.09k_BT$ at a position of 2.33 μm. CG's experiments cannot resolve such small well depths. The attraction in $U(r)$ emerges when charged glass plates were brought closer to a gap less than 6 μm [19,22]. However, the pair potential derived under the DLVO framework for charged colloids with confinement does not show attraction [60]. Similarly, very recent numerical calculations using the Poisson-Boltzmann equation carried out by Ospeck and Fraden [61] for parameters of KF and CG's confined colloids [19,22] also do not show any evidence for attraction. However, these calculations show a reduction in the strength of repulsion. Thus these results clearly suggest that (a) the attraction does not arise due to the physical confinement of charged colloidal particles and (b) confinement does not drastically alter the nature of the interparticle interaction. Hence we believe that the $U_s(r)$ that is derived for bulk suspensions cannot be applied for a quantitative comparison with experimental results of confined colloids. However, we believe that $U_s(r)$ can be used for a qualitative understanding of experimental observations on confined colloids because of our own reported results [20] and from the conclusion drawn above [i.e., (a) and (b)].

We mentioned earlier that the strength of attraction gets enhanced when particles are highly charged. The counterion concentration n_pZ also becomes higher proportionally because the effective charge on the particle dictates the counterion number in the suspension. $U_s(r)$ is derived by taking into account this relationship explicitly [30]. The long-range attractive term in $U_s(r)$ arises due to the mediation of counterions present between charged colloidal spheres [30,37].

We believe that the same counterion mediation is responsible for attraction seen in dilute confined colloids [19,22]. In the case of confined colloids the charge on the glass plates enhances the attraction and the counterions dissociated from the glass plates in addition to those from the particles are responsible for mediating the attraction. It is known that the charge on the glass plate and charge on the colloidal particle comes from similar dissociation processes of respective end chains that are in contact with water. Although the counterion species resulting from the glass plate and the colloidal particle are different, they lose their identity because of their exchange to H^+ by the ion exchange resins. The counterion concentration is expected to reduce when the plate separation is increased. Hence the counterion mediation becomes weak, resulting in an attraction that is too small to be detected when charged plates are at a wider separation. Recent experiments by Muromato *et al.* [58] provide evidence for our explanation. The experiments of Muromato *et al.* with a Nafion-coated polyethylene surface that is charged showed a gathering of similarly charged colloidal particles, whereas experiments with an uncharged polyethylene surface showed no gathering, clearly indicating that a charge on the confined surface and its associated counterions in the suspension are

responsible for the attraction but not the physical confinement. Further, these observations do not support the theoretical results obtained within the framework of the DLVO potential by Gonzalez-Mozuelos and Medina-Noyola [62]. As per these calculations [62], one is expected to observe a piling up of particles touching the wall as the charge density on the similarly charged glass plate is reduced.

CG imagine that the charged glass plates in confined suspensions mimic the role of many colloidal particles in dense suspensions and many-body effects are assumed to be responsible for the origin of attraction seen in bulk suspensions. Many-body effects might be important in concentrated suspensions. However, we do not believe that these are strong enough and responsible for the attraction in dilute suspensions. It is recalled that we observed (a) a vapor-liquid coexistence at a volume fraction as low as 0.000 32 [42], (b) a reentrant transition upon lowering of C_s at a volume fraction 0.0028 [15], and (c) voids coexisting with amorphous dense regions [18] on highly charged colloids at a volume fraction of 0.006. These observations at such low volume fractions cannot be reconciled by many-body effects. However, $U_s(r)$ is shown to explain successfully all these observations, indicating that the influence of counterions present in between the charged colloidal particles is considered reasonably well in deriving the effective pair potential between two colloidal particles in a suspension of finite concentration. Some of these include the present simulations and some have been reported earlier [41,42,18].

Apart from $U_s(r)$, there have been recent calculations based on integral equation methods (IEMs) [28,29] showing the existence of a long-range attraction in the effective pair potential. The behavior of the depth and its position calculated as functions of κ are found to be similar to those of $U_s(r)$. The commonness between IEMs and the Sogami theory is that both consider the finite number of macroions. The Sogami theory explicitly relates the macroion charging process to the release of counterions. However, the DLVO theory is for a very dilute system with no explicit relationship to the macroion charge to the release of counterions. Medina-Noyala and McQuarrie [63] have shown that in the infinite dilution limit IEMs yield the DLVO result. However, such a connection between the Sogami theory and IEMs is yet to be established. Recently, Schmitz [37] reported a thermodynamic picture for the origin of attraction in the Sogami theory by focusing the attention on the electrical part of the Helmholtz and Gibbs free energies and its dependence on the screening parameter κ. He showed that these electrical parts of the two free energies are not equal when κ is finite. This difference is attributed to the internal pressure due to the confinement of the counterions to the vicinity of the macroions. In this context it is worth mentioning the difference between the short-range attraction seen in uncharged colloidal suspensions with free polymer chains and the long-range attraction in charged colloidal suspensions free from any polymer chains. The short-range attraction arises due to the depletion effects when free polymers are present between uncharged colloidal particles [64]. This attraction is of short range because the basic interactions are hard-sphere type. On the other hand, the attraction seen in charged colloids is of long range because the interactions are Coulombic in nature.

VI. CONCLUSIONS

We have shown that the effective interparticle interaction $U_s(r)$, which has a long-range attractive term in addition to the screened Coulomb repulsive term, explains the occurrence of fcc crystalline order at high volume fractions and bcc crystalline order at lower volume fractions. The addition of salt is found to result in melting. For a smaller charge density on particles simulations show a liquidlike order that is found to freeze into a bcc crystalline order upon increasing σ. The variation in volume fraction in the intermediate range also shows a crystal-liquid transition. Thus it is very clear from these simulations that the interparticle interaction need not be repulsive at all interparticle distances to explain the homogeneous phases observed in these suspensions. For suspension parameters for which $R_m > D_0$, the dominant interaction between particles is essentially repulsive and responsible for the homogeneous nature of the suspension and the ordering is dictated by the strength of interaction at D_0. This explains why $U_s(r)$ is equally successful in explaining the structural order in homogeneous suspensions, which is otherwise explained using the DLVO potential. For those suspensions where $R_m < D_0$ simulations showed a vapor-liquid coexistence for low values of σ and ϕ. This coexisting state is found to transform into a homogeneous liquid state beyond a critical value of ϕ, in agreement with the experimental observations. For large values of σ the well depths are large, resulting in the formation of voids with ordered or disordered structures. At very dilute volume fractions simulations showed a concentration-independent single peak, which is in conformity with experimental observations. The present simulations explain several experimental observations, viz., the direct measurement of the pair potential, the vapor-liquid coexistence to a homogeneous liquid state upon variation of ϕ, and the coexistence of voids with ordered and disordered regions. These cannot be understood based purely on the repulsive DLVO potential. In view of the present simulation results, the earlier understanding obtained using the DLVO potential to explain the bcc-fcc transition and the melting phenomena needs a revision.

The present simulations clearly emphasize the importance of the κ-dependent long-range attractive term in the interparticle interaction for the description of ordering phenomena in charged colloids. *Ab initio* calculations are expected to provide insight into the mechanism of the long-range attraction and also help in resolving the existing debate [1,31,32,34–37] on the validity of the Sogami theory [30]. Careful experiments on very dilute suspensions of highly charged particles under unconfined geometry help in the understanding of the origin of the long-range attraction.

ACKNOWLEDGMENTS

We thank Dr. A. K. Arora and Professor I. Sogami for useful suggestions. Financial support for this work as well as the stay of B.V.R.T. at Osaka, given by Rengo Company Limited, Osaka, Japan, is gratefully acknowledged.

[1] For recent reviews, see *Ordering and Phase Transitions in Charged Colloids*, edited by A. K. Arora and B. V. R. Tata (VCH, New York, 1996).
[2] P. L. Flaugh, S. E. O'Donnell, and S. A. Asher, Appl. Spectrosc. **38**, 847 (1984); S. A. Asher, P. L. Plaugh, G. Washinger, Spectroscopy **1**, 26 (1986); H. B. Sunkara, J. M. Jethmalani, and W. T. Ford, Chem. Mater. **6**, 362 (1994).
[3] I. I. Buhan and G. H. Watson, Phys. Rev. Lett. **76**, 315 (1996).
[4] E. J. W. Verwey and J. Th. G. Overbeek, *Theory of the Stability of Lyophobic Colloids* (Elsevier, Amsterdam, 1948).
[5] N. Ise, in *Ordering and Organization in Ionic Solutions*, edited by N. Ise and I. Sogami (World Scientific, Singapore, 1988), p. 624.
[6] R. Kesavamoorthy, M. Rajalakshmi, and C. Babu Rao, J. Phys.: Condens. Matter **1**, 7149 (1989).
[7] S. Dosho *et al.* Langmuir **9**, 394 (1993).
[8] K. Ito, H. Yoshida, and N. Ise, Science **263**, 66 (1994).
[9] H. Yoshida, N. Ise, and T. Hashimoto, J. Chem. Phys. **103**, 10 146 (1995).
[10] N. Ise and H. Yoshida, Acc. Chem. Res. **29**, 3 (1996).
[11] N. Ise, K. Ito, H. Matsuoka, and H. Yoshida, in *Ordering and Phase Transitions in Charged Colloids* (Ref. [1]), p. 101.
[12] A. K. Arora and R. Kesavamoorthy, Solid State Commun. **54**, 1047 (1985).
[13] N. Ise, T. Okubo, M. Sugimura, K. Ito, and H. J. Nolte, J. Chem. Phys. **78**, 536 (1983); Adv. Polym. Sci. **114**, 187 (1994).
[14] T. Konishi, N. Ise, H. Matsuoka, H. Yamaoka, I. Sogami, and T. Yoshiyama, Phys. Rev. B **51**, 3914 (1995); T. Konishi and N. Ise, J. Am. Chem. Soc. **117**, 8422 (1995).
[15] A. K. Arora, B. V. R. Tata, A. K. Sood, and R. Kesavamoorthy, Phys. Rev. Lett. **60**, 2438 (1988).
[16] B. V. R. Tata, M. Rajalakshmi, and A. K. Arora, Phys. Rev. Lett. **69**, 3778 (1992); T. Palberg and M. Wurth, *ibid.* **72**, 786 (1994); B. V. R. Tata and A. K. Arora, *ibid.* **72**, 787 (1994).
[17] K. Ito, H. Nakamura, H. Yoshida, and N. Ise, J. Am. Chem. Soc. **110**, 1955 (1988); A. E. Larsen and D. G. Grier, Phys. Rev. Lett. **76**, 3862 (1996); Nature (London) **385**, 230 (1997).
[18] B. V. R. Tata, E. Yamahara, P. V. Rajamani, and N. Ise, Phys. Rev. Lett. **78**, 2660 (1997).
[19] G. M. Kepler and S. A. Fraden, Phys. Rev. Lett. **73**, 356 (1994).
[20] B. V. R. Tata and A. K. Arora, Phys. Rev. Lett. **75**, 3200 (1995).
[21] M. D. Carbjal-Tinoco, F. Castro-Roman, and J. L. Arauz Lara, Phys. Rev. E **53**, 3745 (1996).
[22] J. C. Crocker and D. G. Grier, Phys. Rev. Lett. **77**, 1897 (1996).
[23] K. Vondermassen, J. Bongers, A. Mueller, and H. Versmold, Langmuir **10**, 1351 (1994).
[24] J. C. Crocker and D. G. Grier, Phys. Rev. Lett. **73**, 352 (1994).
[25] Bo Jönsson, T. Åkesson, and C. E. Woodward, in *Ordering and Phase Transitions in Charged Colloids* (Ref. [1]), p. 296.
[26] M. J. Stevens, M. L. Falk, and M. O. Robbins, J. Chem. Phys. **104**, 5209 (1996).
[27] O. Spalla and L. Belloni, Phys. Rev. Lett. **74**, 2515 (1995).
[28] X. Chu and D. T. Wasan, J. Colloid Interface Sci. **184**, 268 (1996).
[29] M. D. Carbajal-Tinoco, and D. G. Grier (unpublished).
[30] I. Sogami, Phys. Lett. **96A**, 199 (1983); I. Sogami and N. Ise, J. Chem. Phys. **81**, 6320 (1984).
[31] J. Th. G. Overbeek, J. Chem. Phys. **87**, 4406 (1987).
[32] C. E. Woodward, J. Chem. Phys. **89**, 5140 (1988).
[33] N. Ise, H. Matsuoka, K. Ito, H. Yoshida, and J. Yamanaka, Langmuir **6**, 296 (1990), footnote 32.
[34] M. V. Smalley, Mol. Phys. **71**, 1251 (1990); see also *Ordering and Phase Transitions in Charged Colloids* (Ref. [1]), p. 315.
[35] K. S. Schmitz, *Macroions in Solution and Colloidal Suspension* (VCH, New York, 1993).
[36] K. S. Schmitz, Acc. Chem. Res. **29**, 5 (1996).
[37] K. S. Schmitz, Langmuir **12**, 1407 (1996); **12**, 3828 (1996).
[38] B. V. R. Tata, A. K. Sood, and R. Kesavamoorthy, Pramana **34**, 23 (1990).
[39] K. Ito, K. Sumaru, and N. Ise, Phys. Rev. B **46**, 3105 (1992).
[40] N. Ise and M. V. Smalley, Phys. Rev. B **50**, 16 722 (1994).
[41] B. V. R. Tata, A. K. Arora, and M. C. Valsakumar, Phys. Rev. E **47**, 3404 (1993).
[42] B. V. R. Tata and N. Ise, Phys. Rev. B **54**, 6050 (1996).
[43] K. Binder, in *Monte Carlo Methods in Statistical Physics*, edited by K. Binder (Springer-Verlag, New York, 1979), p. 1.
[44] B. V. R. Tata, Ph.D. thesis, University of Madras, 1992 (unpublished).
[45] B. V. R. Tata, A. K. Arora, J. Phys.: Condens. Matter **3**, 7983 (1991); **4**, 7699 (1992); **7**, 3817 (1995).
[46] J. P. Hansen and I. R. McDonald, *Theory of Simple Liquids* (Academic, London, 1986).
[47] E. B. Sirota, H. D. Ou-Yung, S. K. Sinha, P. M. Chaikin, J. D. Axe, and Y. Fujji, Phys. Rev. Lett. **62**, 1524 (1989).
[48] R. O. Rosenberg and D. Thirumalai, Phys. Rev. A **36**, 5690 (1987); D. Thirumalai, J. Phys. Chem. **93**, 5637 (1989).
[49] M. O. Robbins, K. Kremer, and G. S. Grest, J. Chem. Phys. **88**, 3286 (1988).
[50] D. Hone, S. Alexander, P. M. Chaikin, and P. Pincus, J. Chem. Phys. **79**, 1474 (1983).
[51] S. Sengupta and A. K. Sood, Phys. Rev. A **44**, 1233 (1991); J. Chakrabarti, H. R. Krishanmoorthy, S. Sengupta, and A. K. Sood, in *Ordering and Phase Transitions in Charged Colloids* (Ref. [1]), p. 235.
[52] J. P. Hansen and L. Verlet, Phys. Rev. **184**, 150 (1969).
[53] F. A. Lindemann, Z. Phys. **11**, 609 (1934).
[54] J. Yamanaka, T. Koga, N. Ise, and T. Hashimoto, Phys. Rev. E **53**, R4314 (1996); J. Yamanaka, H. Hayashi, N. Ise, and T. Yamguchi, *ibid.* **55**, 3028 (1997).
[55] R. van Roij and J. P. Hansen, Phys. Rev. Lett. **79**, 3082 (1997).
[56] D. A. McQuarrie, *Statistical Mechanics* (Harper & Row, New York, 1973).
[57] J. Yamanaka and N. Ise (private coummunication).
[58] T. Muromato, K. Ito, and H. Kitano, J. Am. Chem. Soc. **119**, 3592 (1997).
[59] S. Yoshino, Polym. Int. **30**, 541 (1993).
[60] E. Chang and D. W. Hone, Europhys. Lett. **5**, 635 (1984).
[61] M. Ospeck and S. Fraden (unpublished).
[62] P. Gonzalez-Mozuelos and M. Medina-Noyola, J. Chem. Phys. **94**, 1480 (1991); **93**, 2109 (1990).
[63] M. Medina-Noyola and D. A. McQuarrie, J. Chem. Phys. **73**, 6279 (1980).
[64] S. Asakura and F. Oosawa, J. Chem. Phys. **22**, 1255 (1954); J. Polym. Sci. **33**, 183 (1958).